Scripta Materialia xxx (2016) xxx–xxx

Contents lists available at ScienceDirect

Scripta Materialia

journal homepage: www.elsevier.com/locate/scriptamat

Viewpoint article

Opportunities and limitations for ion beams in radiation effects studies: Bridging critical gaps between charged particle and neutron irradiations

S.J. Zinkle [a,b,*], L.L. Snead [c]

[a] University of Tennessee, Knoxville, TN 37996, USA
[b] Oak Ridge National Laboratory, Oak Ridge, TN 37831, USA
[c] State University of New York, Stony Brook, NY, USA

ARTICLE INFO

Article history:
Received 29 May 2017
Received in revised form 22 June 2017
Accepted 22 June 2017
Available online xxxx

Keywords:
Irradiation effects
Ion irradiation
Microstructure
Injected intersititials
Metals

ABSTRACT

Ion beams are indispensible for understanding radiation effects in materials, enabling access to conditions challenging to perform with neutrons. However, ion irradiations can produce potential artifacts from beam rastering, high displacement damage rate effective "temperature shifts", subthreshold collisions, high ionization rates, and non-monoenergetic primary knock-on atom energies. The influence of near-surface denuded zones and implanted ion effects is analyzed, including diffusional broadening effects. At high ion irradiation energies, "swift heavy ion" effects can lead to enhanced defect production or recovery. Ion energies of 10–50 MeV typically offer a good compromise for minimizing near-surface, implanted ion, and swift heavy ion effects.

1. Advantages of ion beams for radiation effects research

Charged particle irradiation studies have been utilized for understanding irradiation effects on the microstructure and microchemistry in materials for many decades [1–3]. It is well established that ion irradiations can reproduce essentially all of the standard microstructural features observed in neutron-irradiated materials (dislocation loops, cavities, radiation-induced solute segregation, radiation-induced precipitation, etc.). Charged particle irradiations are a valuable complementary tool to bulk neutron irradiation studies, and in many cases provide unique capabilities to explore radiation effects phenomena. In particular, they allow the possibility to carefully and systematically control irradiation conditions over a wide range of doses in order to explore important test conditions such as exposure temperature, dose rate (including pulsed irradiation effects) and primary knock-on atom (PKA) energy. High displacement damage levels of ~100 displacements per atom (dpa) or higher can be achieved rapidly at relatively low cost with average PKA energies comparable to that of neutron or fission fragment irradiations, with little or no induced radioactivity [4,5]. Ion beams provide opportunities for improved experimental control that are difficult or impossible to perform during reactor neutron irradiations such as separate effects testing. For example, simultaneous dual or triple ion beam studies can quantify the roles of helium and hydrogen transmutation products on microstructural evolution during irradiation [6]. The thermal control region is located immediately adjacent to the irradiated region in the same sample, enabling quantitative differentiation of thermal- vs. radiation-induced microstructural changes.

The capability to produce controlled amounts of displacement damage under well-defined experimental conditions enables ion irradiations to be the preferred approach over neutron irradiations for many fundamental radiation effects studies. The length scale of the irradiation damage region for ion beams with MeV energies (~1 μm) is sufficiently large to extract microstructural information relevant for bulk irradiation conditions. By utilizing cross-section analysis techniques, the depth dependence of the damage rate and cumulative damage level can in principle be used to explore multiple dose rates and damage levels within a single fluence specimen. The near-atomic-scale resolution now achievable in modern electron microscopes and atom probe tomography allows chemical and defect cluster information to be obtained on scales comparable to that from modeling and simulation studies such as molecular dynamics. Valuable depth-dependent structural and chemical information can also be obtained from a variety of Rutherford spectrometry, nuclear reaction analysis [7], and/or glancing incidence x-ray diffraction measurements. In addition, technology improvements in time-dependent "4-dimensional" transmission electron microscopy [8] and synchrotron x-ray sources [9] enable valuable kinetic information to be obtained from in-situ ion irradiation studies in specialized facilities where the ion beams are linked to an electron microscope [10] or synchrotron beam line. Important defect production information can be obtained from analysis of bulk vs. thin foil ion irradiated specimens [11,12]. Similarly, ion beam irradiations can enable important experimental

* Corresponding author.
E-mail address: szinkle@utk.edu (S.J. Zinkle).

http://dx.doi.org/10.1016/j.scriptamat.2017.06.041
1359-6462/

validation of fundamental radiation effects processes, such as confirmation of molecular dynamics simulations of glissile defect clusters that may exhibit one-dimensional migration [13,14].

2. Limitations of ion beams for investigating neutron radiation effects

These important experimental benefits can be contrasted with a number of well-known limitations associated with ion beam irradiations that require careful data interpretation. Due to the limited penetration depth of ion beams in materials it is difficult to extract bulk property information from the irradiated region beyond microstructural and microchemical information, although promising improvements in nanoscale thermal conductivity [15–18] and mechanical property [19,20] techniques are under development.

A general limitation of ion beam irradiations is that the PKA recoils are distributed over a relatively wide range of energies compared to neutron irradiations, with most of the collisions producing low energy recoils due to long-range Coulombic interactions. For example, over 80% of the PKAs have energies <1 keV for 1 MeV self ion irradiation of medium mass targets such as Cu or Fe whereas the maximum PKA energy extends up to 1 MeV; in contrast, about 80% of the PKAs from 1 MeV neutron irradiation have energies within a factor of two of the maximum PKA energy of ~60 keV [21]. Therefore, near-monoenergetic PKA irradiations generally cannot be achieved using ion beams. Fig. 1 summarizes molecular dynamics simulations of the calculated surviving defect fraction (normalized to the NRT dpa) versus PKA energy for displacement events in Fe at 100 K [22]. The inset figure summarizes the calculated weighted defect recoil spectra W(T) versus PKA energy for 1 MeV neutrons and several ions in Cu, where W(T) is defined as the fraction of displacement damage produced in recoils of energy T [21]. The displacement events for ion irradiation occur over a wider energy range compared to neutrons, with a significantly higher fraction of low-energy and high-energy recoil events for the same average value of W(T). For example, ~20% and ~40% of the calculated displacement damage in Cu is associated with PKA energies below 10 keV for 1 MeV Kr and Ne ions, respectively, compared to <2% for 1 MeV neutrons. Whereas the surviving defect fraction is approximately constant at high PKA energies due to onset of subcascade formation [22] (>10 keV for medium-mass targets such as Fe, cf. Fig. 1), it increases rapidly at low PKA energies. Overall, the larger fraction of low energy PKAs for ion irradiation compared to neutron irradiation produces smaller-sized defect clusters created directly within displacement cascade events (with potentially different stability and mobility) and a higher surviving defect fraction per dpa compared to neutron irradiations.

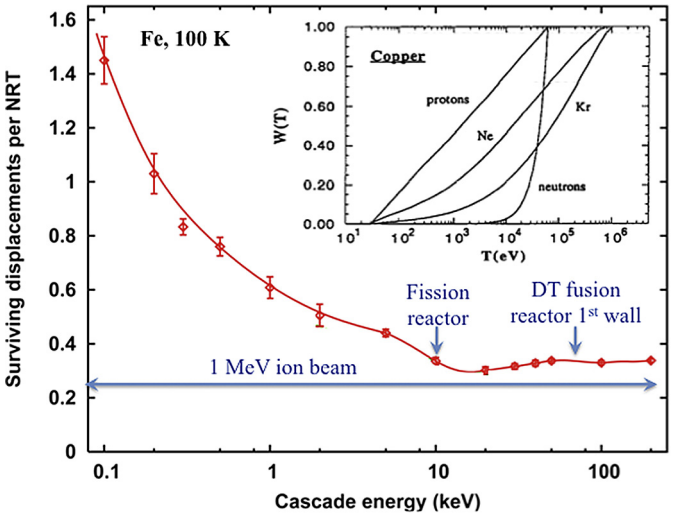

Fig. 1. Calculated surviving defect fraction (normalized to the NRT dpa) versus PKA energy for displacement events in Fe at 100 K [22]. The inset figure summarizes the calculated weighted defect recoil spectra W(T) versus PKA energy for several 1 MeV light ions and neutrons in Cu [21].

Energetic ion beams (>1 MeV) also produce high amounts of ionization per displaced atom along with an increased proportion of very low collisional energy transfers (below the threshold for stable displacement damage) compared to neutrons. These high ionization and subthreshold collision energy processes may cause pronounced increases in defect diffusion and point defect recombination relative to neutron irradiation conditions [23–29], particularly for energetic light ions. Since the energy transfer associated with subthreshold collisions (i.e., up to ~25–40 eV) is much higher than typical defect migration energies (~1 eV), subthreshold collisions can stimulate enhanced point defect migration and recombination in all irradiated materials [28,29]. However, further research is needed to quantify the importance of subthreshold collisions on defect evolution under a wide variety of irradiation conditions. The high amount of ionization per dpa for ion compared to neutron irradiations can also produce potentially dramatic reductions in surviving defect production in nonmetals such as semiconductors and ceramic insulators [23–27]. <10% of the energy loss of ~1 MeV medium-mass ions is associated with displacement damage collisions (with the majority energy loss associated with electron/ionization interactions), vs. approximately equal magnitudes of electronic and nuclear stopping powers for PKAs associated with neutron collisions. The ratio of ionization to nuclear stopping power increases with decreasing mass and increasing ion energy above ~1 MeV [23]. Ionizing radiation environments up to electronic stopping powers of ~10 keV/nm are typically of no consequence in metals due to their high concentration of conduction electrons, but can produce dramatic microstructural differences such as pronounced defect cluster coarsening or inhibition of amorphization in semiconductors and insulators compared to low ionization per dpa irradiation conditions [23–27].

An important advance in accelerator technology over the past few decades is the capability to raster a finely focused ion beam in order to achieve uniform irradiation fluences over the exposed area. However, the use of rastered or pulsed beams (frequencies of 0.1–250 Hz) has been shown in several experimental studies to lead to suppressed void swelling at intermediate temperatures [30–33]. Modeling studies indicate that the irradiation pulsing associated with beam rastering can alter the microstructural evolution, with effects most pronounced at pulse frequencies near ~1–100 Hz at intermediate temperatures [32–34]; the beam pulsing effect is predicted to disappear at very high pulse frequencies. Although further experimental and modeling studies are needed to quantify the material-, dose rate- and temperature-dependent conditions where beam pulsing effects become significant, it is recommended that defocused beams should generally be used instead of rastered beams for irradiation effects studies at elevated temperatures. Some slight electromagnetic wobbling of a defocused beam (where the ion flux at a given position never falls below ~50% of the peak flux) may be an alternative to provide a more uniform fluence over broad irradiated regions.

In order to take advantage of the high dose rate (which varies with depth) for typical ion irradiations, careful experimental planning and interpretation is required to enable quantitative comparison with neutron irradiation (lower dose rate) conditions. For example, in order to achieve comparable defect arrival rates at features such as sinks or defect cluster nuclei, high dose rate irradiations must be performed at higher temperature compared to low dose rate irradiations [35,36]. Unfortunately, this quantitative "temperature shift" is predicted to vary for different microstructural features (e.g., voids, interstitial dislocation loops, precipitates), since they depend on rate-controlling processes such as vacancy or solute migration with different thermal activation energies. Furthermore, kinetic rate theory analyses [32] predict a different functional dependence when trying to achieve equivalent point defect arrival fluxes at sinks versus when trying to achieve equivalent dislocation loop concentrations; in general, these analyses indicate no

Please cite this article as: S.J. Zinkle, L.L. Snead, Opportunities and limitations for ion beams in radiation effects studies: Bridging critical gaps between charged particle and neut..., Scripta Materialia (2016), http://dx.doi.org/10.1016/j.scriptamat.2017.06.041

single "temperature shift" can be used to correlate irradiations performed at different dose rates [37]. The dose rate effect also changes its functional form for recombination-dominant (low temperature) irradiations compared to sink-dominant (high temperature) irradiations [36], and is expected to follow different functional dependencies for the nucleation vs. growth phases of microstructural evolution. Nevertheless, it is worth noting that some limited studies have reported relatively good quantitative agreement between ion and neutron irradiations for multiple microstructural features (voids, dislocation loops, G phase precipitates) using a single temperature shift for the high dose rate ion irradiated ferritic/martensitic steel [38]. Further experimental and modeling studies are needed to comprehensively quantify the effect of dose rate and irradiation temperature on the microstructural evolution of cavities, precipitates, dislocation loops, and network dislocations. An additional consideration is that a limited number of neutron [39–41] and ion [42,43] irradiation studies on austenitic [39–42] and ferritic/martensitic [43] steels have reported that void swelling at a given dose decreases with increasing dose rate due to a lengthening of the transient low-swelling regime. However, the reported dose rate dependence of the transient low-swelling regime is inconsistent between the neutron and ion irradiation data sets (e.g., no swelling in Fe-Cr-Ni austenitic alloys would be predicted for 10^{-3} dpa/s ion irradiations up to 1000 dpa based on extrapolation of the neutron dose rate database). Therefore, extrapolation of void swelling results from high dose rate ion irradiations to neutron-relevant conditions is challenging due to current limitations in quantitative understanding of dose rate effects. This would be a profitable area for additional research.

For high beam flux experiments, it is important to utilize appropriate thermal management procedures (good thermal contact of the samples to temperature-controlled heat sinks) and continuous surface temperature monitoring to accurately control and measure the specimen irradiation temperature. For medium-mass MeV ion beams the deposited heat flux associated with irradiations at ~10^{-3} dpa/s corresponds to a few W/cm^2, which is on the order of the heat applied by furnaces for intermediate temperature ion irradiations.

3. Near-surface and implanted ion effects

A defect-depleted zone is typically observed in irradiated materials due to the reduction of point defect supersaturation in the vicinity of planar sinks such as grain boundaries or free surfaces. Near-surface defect depletion is observed for both interstitial- (e.g., dislocation loops) [44–46] and vacancy-type defect clusters (e.g., voids) [2,30,31,43,47–49]. For recombination-dominant conditions typical for void swelling the denuded zone width is proportional to $(D_v/P)^{1/4}$ where D_v is the vacancy diffusivity and P is the damage rate, whereas for sink-dominant conditions the denuded zone width is proportional to $C_s^{-1/2}$ where C_s is the sink density [50,51]. Several researchers have reported a localized peak void swelling regime at depths immediately adjacent to the denuded zone at free surfaces or along grain boundaries [52–56]. This peak swelling zone has been attributed to localized interstitial depletion as a result of longer interaction mean free paths for interstitial defect clusters due to one-dimensional glide (vs. predominantly 3-dimensional random walk diffusion for vacancies) [57,58] or other mechanisms causing biased loss of interstitials to the surface [59,60], or alternatively due to spatially-varying dislocation densities near planar sinks [61]. Similar near-surface enhancement of vacancy dislocation loop size and density has been attributed to preferential loss of self-interstitial atoms to the surface [62]. The width of the near-surface depleted zone should be routinely reported and this region should be always excluded from ion-neutron correlation evaluations. If evidence of an adjacent "peak zone" for defect cluster formation or growth is detected, this peak zone should also be reported and excluded from quantitative ion-neutron correlation analysis.

The bombarding ions are deposited in a subsurface region near the peak displacement damage region, where they may exert chemical and/or excess-interstitial defect imbalance effects. Significant implanted ion effects have been reported regarding enhanced amorphization of ceramics [63–66], modified dislocation loop evolution in metals and ceramics [46,63,67], reduced alpha prime precipitate formation in Fe-Cr alloys [68], and suppression of void swelling in numerous metals [31,35,43,48,49,69–73]. Besides possible chemical effects, the implanted ion region introduces a localized excess of interstitial atoms, which creates an imbalance in the normal vacancy and interstitial supersaturation concentrations [60,70,73–76]. For recombination-dominant conditions (low to intermediate temperatures), pronounced effects on void nucleation in face centered cubic metals such as Ni are calculated to occur for injected ion concentrations $\varepsilon_i > 10^{-4}$ atom fraction per dpa [73,75,76]. The implanted ion concentration profile at temperatures where defects are immobile is approximately Gaussian and is readily calculated using computer codes such as SRIM [77], but at elevated temperatures diffusional broadening of the implanted ion profile due to thermal and radiation-enhanced diffusion [48,78–80] must be considered, which will preferentially induce diffusion of the implanted ions toward the surface [48].

Since the near-surface and implanted-ion zones can dramatically modify the local microstructure during ion irradiation, the depth-dependent microstructure should be examined over the entire ion range to confirm the existence of suitable "safe zones" and microstructural characterization must generally be performed at these intermediate "safe zone" depths to avoid these artifacts. Fig. 2 summarizes examples of the near-surface and implanted ion effects on the interstitial dislocation loop microstructure for 2 MeV Al^+ ion irradiated $MgAl_2O_4$ ceramic at 650 °C for irradiation at the same flux to two fluences that vary by a factor of 8 [46,63]. A dislocation loop denuded zone is observed within

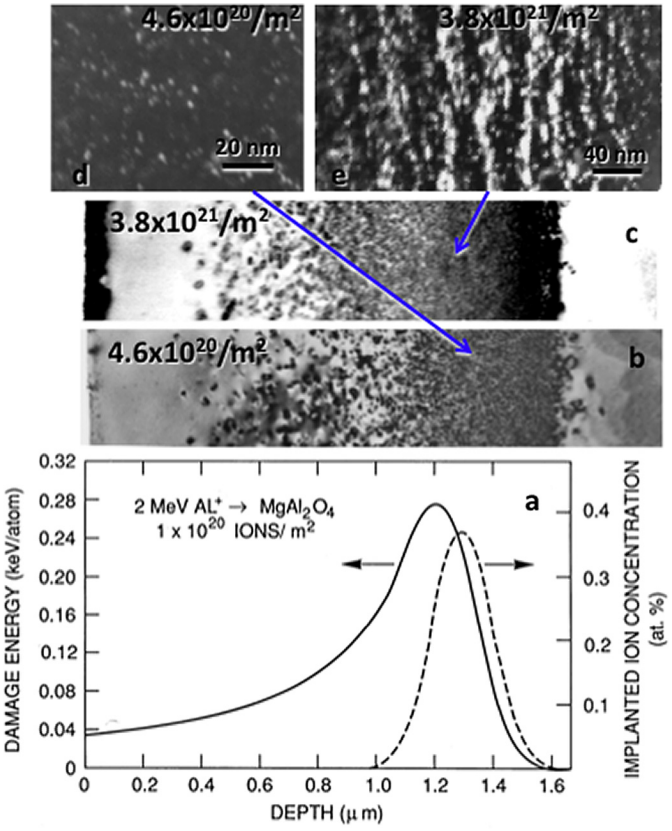

Fig. 2. Calculated displacement damage and implanted ion profiles for 2 MeV Al^+ ions in $MgAl_2O_4$ (a) [46,63] compared to observed cross-section TEM images after 4.6×10^{20}/m^2 (b) [46,63] and 3.8×10^{21}/m^2 (c) [46] at 650 °C. Assuming a sublattice-averaged displacement energy of 40 eV, these fluences produce peak damage levels of ~14 and 101 dpa, respectively. Metallic Al colloid precipitates are visible as white contrast features in d, e) [63,81] for implanted ion concentrations >0.2 at.%.

Please cite this article as: S.J. Zinkle, L.L. Snead, Opportunities and limitations for ion beams in radiation effects studies: Bridging critical gaps between charged particle and neut..., Scripta Materialia (2016), http://dx.doi.org/10.1016/j.scriptamat.2017.06.041

~0.4 μm from the irradiation surface at both fluences. The microstructure in the ion implanted region is significantly affected by metallic Al colloid precipitation [63,81] for implanted ion concentrations >0.2 at.%. In particular, dislocation loops visible in the midrange region (~0.4–1 μm depths) are replaced with network dislocations and metallic precipitates in the implanted ion region (~1.1–1.6 μm depths) of the lower fluence sample for damage levels of ~5–14 dpa. This conversion of dislocation loops to network dislocations did not occur outside of the implanted ion region for damage levels up to at least ~30 dpa, as demonstrated in the midrange regions (~0.5–1 μm depths) of the higher fluence sample in Fig. 2c.

For elevated-temperature ion irradiations exploring phenomena such as void swelling, the ion energy needs to be sufficiently high to enable analysis to be performed in a midrange region (>0.2–0.4 μm wide) that is well separated from the near-surface (denuded and peak swelling regions) and implanted ion zones. For example, the reported peak void swelling temperature is 450-480 °C for ferritic/martensitic (FM) steels irradiated with Fe ions at a dose rate near 10^{-3} dpa/s [43,82–84]. Prior ion-irradiated FM steel studies have observed significant near-surface void swelling suppression at 450–475 °C at depths within ~400 nm from the surface [30,31,43,49,85]. This surface-affected zone increases with increasing irradiation temperature [48,50,86,87]. Regarding implanted ion effects, FM steel ion irradiation studies at 450-475 °C have observed pronounced void swelling suppression due to implanted ions for irradiated midrange regions located as far as ~600–800 nm from the calculated peak implantation depth [30,31,43,49,85]. This corresponds to calculated as-implanted ion concentrations of $\varepsilon_i \sim 2 \times 10^{-5}$/dpa, but the actual excess Fe concentration at this depth will be larger due to diffusional broadening (thermal and radiation-enhanced) that will preferentially cause diffusion of the implanted Fe toward the irradiated surface [48].

Fig. 3 shows the calculated temperature-dependent void denuded zone near the surface and the injected ion-affected region ($\varepsilon_i > 10^{-4}$/dpa) for 5 MeV Fe ion irradiated Fe-10%Cr at midrange doses of 50–500 dpa (projected ion range ~1500 nm, range straggling ~230 nm). For simplicity, surface sputtering effects were ignored [88]. The dose-independent near-surface void denuded zone width Δx_v was calculated assuming recombination-dominant conditions using $\Delta x_v \sim (D_v/P)^{1/4} \sim [\exp(-E_{vm}/4kT)]/P^{1/4}$, where E_{vm} is the vacancy migration energy (0.7 eV) and P is the damage rate [50,51]. We assumed a constant ion beam damage rate (10^{-3} dpa/s) with a corresponding radiation enhanced diffusion coefficient for FM steel at ~500 °C of $D_{red} = 1 \times 10^{-18}$ m^2/s [89], and used a smoothly varying $D_{red} = 1 \times 10^{-20}$ to 4×10^{-18} m^2/s between 227 °C and 627 °C to account for temperature dependence [78,79]. The precise D_{red} value would depend on the defect sink strength evolution during irradiation associated with precipitates and other microstructural features. Depth-dependent variations in the dose rate were ignored. The as-implanted Fe ion concentration profile was calculated using SRIM [77], and subsequent diffusional broadening was analytically estimated using Eq. (1), which is the solution to Fick's 2nd law for a constant flux ϕ_0 of implanted solute in a semi-infinite solid, where C is the solute concentration, N_{at} is the host atomic concentration, t is time and x is the diffusion distance from the initial injected solute location [90]:

$$C = \frac{2\varphi_0\sqrt{D_{red}t}}{N_{at}D_{red}}\left\{\frac{exp\frac{-x^2}{4D_{red}t}}{\sqrt{\pi}} - \frac{x}{2\sqrt{D_{red}t}}\ erfc\frac{x}{2\sqrt{D_{red}t}}\right\} \quad (1)$$

From the SRIM as-implanted ion distribution, the injected Fe solute exceeds $\varepsilon_i = 10^{-4}$/dpa for depths between 1040 and 1725 nm due to range straggling. Radiation enhanced diffusion during the implantation causes the implanted ion profile to broaden preferentially toward the surface with increasing dose and temperature. The diffusion-broadened injected solute exceeds $\varepsilon_i = 10^{-4}$/dpa at progressively shallower depths with increasing dose and temperature. At an irradiation temperature of 450–500 °C (relevant for void swelling studies in ion irradiated FM steels), a midrange region at depths ~450–900 nm is calculated to be relatively unaffected by near-surface or implanted ion effects for a dose of 50 dpa. However, as the dose increases to 500 dpa there is essentially no midrange region that is not affected by either near-surface or implanted ion effects at 450-500 °C. The quantitative accuracy of the predicted broadening of the injected ion region in Fig. 3 is contingent on the assumed radiation enhanced diffusion values and the relevant critical injected ion concentration for suppressing void nucleation and growth (each of which are poorly quantified for FM steels). Further research to better quantify these fundamental parameters would be valuable for improved estimates of safe analysis zones.

The predictions summarized in Fig. 3 are in general agreement with depth-dependent void swelling data for 3.5–5 MeV Fe ion irradiated FM steels: Although the data exhibit some variability due to generally low overall void swelling, the reported swelling is often sharply peaked in a narrow range of depths near 500–800 nm [30,31,43,49,85], suggesting pronounced near-surface and injected ion suppression of void swelling at shallower and deeper depths, respectively. Analyses similar to that used to construct Fig. 3 predict that self-ion energies below 5 MeV would yield progressively smaller midrange regions suitable for artifact-free characterization. For example, for Fe ion energies ≤2 MeV (implanted ion range ~ 700 nm) there is predicted to be no irradiated region that would not be affected by either near-surface or implanted ion effects at 450-500 °C even at relatively low doses of ~50 dpa and, for commonly used Fe ion energies of 3.5–4 MeV, implanted ion or near-surface artifacts are predicted to occur at all irradiation depths for doses above ~200 dpa. The reported high dose steady state swelling rates for FM steels such as HT9 and 9Cr—1Mo Alloy 91 following 3.5–5 MeV self ion irradiation [30,43,49,84,85] are generally lower than observed after neutron [91] irradiation (0.033 to 0.08%/dpa for ions vs. ~0.2%/dpa for neutrons). Although there are several possible contributing factors including damage rate and/or transmutant He effects, Fig. 3 predicts that surface and/or injected ion effects may be contributing to the observed lower void swelling rates in these 3.5–5 MeV high dose ion irradiation studies.

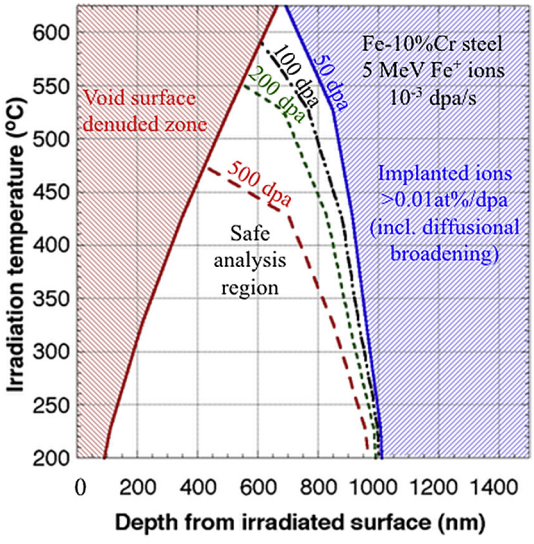

Fig. 3. Calculated temperature- and depth-dependent regions affected by the free surface and injected ions for Fe-10%Cr steel irradiated with 5 MeV Fe^+ ions at 10^{-3} dpa/s to dose levels of 50–500 dpa. A relatively wide analysis region exists between the surface-affected and injected ion-affected regions at 50 dpa (400–900 nm depths near the peak swelling temperature of 450 °C), but diffusional broadening causes this safe analysis region to disappear at higher doses and temperatures.

Please cite this article as: S.J. Zinkle, L.L. Snead, Opportunities and limitations for ion beams in radiation effects studies: Bridging critical gaps between charged particle and neut..., Scripta Materialia (2016), http://dx.doi.org/10.1016/j.scriptamat.2017.06.041

4. Tradeoffs in optimized ion beam energy for exploring neutron radiation effects

One obvious approach to provide a broader midrange irradiation region unaffected by near-surface or implanted ion effects is to increase the ion energy. For example, increasing the Fe ion energy to 9 MeV (mean range of 2.7 μm) for the analysis summarized in Fig. 3 would provide over 1 μm additional separation between the surface- and implanted ion-affected regions compared to 5 MeV ions. However, the ion energy cannot be increased indefinitely since at very high ion irradiation energies new radiation effects phenomena associated with intense localized ion track ionization emerge in addition to traditional knock-on displacement damage. These "swift heavy ion" effects have been observed to occur in metals [92–98], semiconductors [99–101] and inorganic insulators [102–107] above material- and ion velocity-dependent threshold values for electronic stopping power of ~1–50 keV/nm. A wide variety of new radiation-induced phenomena associated with the intense ion track ionization have been observed within or adjacent to the ion tracks, including enhanced defect production (point defects and defect clusters), enhanced annealing of defects produced by conventional knock-on displacement damage, and phase transformations including crystalline-crystalline, crystalline to amorphous, and amorphous to crystalline. Since the radiation-induced phenomena associated with swift heavy ions involve different physical mechanisms for defect production and radiation-enhanced recombination compared to conventional displacement damage, interpretation of swift heavy ion experimental data for prediction of neutron irradiation behavior is problematic. In materials with a high threshold for ion track damage, swift heavy ion effects may be negligible for self-ion irradiations up to ~1 GeV due to insufficiently intense ionization to induce track damage (in these cases, track damage can only be induced using very heavy ions or ion cluster beams). However, in general for medium mass materials the self-ion energy associated with the onset of swift heavy ion effects is typically in the range of 50 MeV (radiation-sensitive materials) to several hundred MeV (moderate ion track sensitivity).

To date the preponderance of ion-beam irradiation studies on materials have been performed at either relatively low energy (<100 keV near-surface implantation supporting, e.g., the electronics industry or surface modification technologies) or at intermediate energy (0.1–5 MeV, for a variety of irradiation material science and nuclear technology objectives). A minority of fundamental and applied studies have utilized high-energy ion beams, including those related to light ion irradiation and He implantation studies [108–110], spallation radiation effects research [111–113], nuclear fuels [114,115] and inert matrix fuel hosts or ceramic waste forms [107,116–118]. The relative lack of studies using high energy ions is in part associated with historical accelerator facility capability and cost considerations. Low energy high beam current ion implanters are low cost and therefore widely deployed, particularly for industrial applications. Intermediate energy ion accelerator facilities serve a variety of scientific purposes for physics and materials science research; typical tandem accelerators with dome voltages of 1–5 MeV are commonplace at universities and research institutions and can enable irradiation studies at ion energies of ~1–25 MeV depending on the selected ion charge state (accelerated beam current decreases with increasing ion charge state due to the lower probability of producing highly ionized ions). In order to access high energy ion irradiations, historically expensive cyclotrons or other large scale, costly accelerators were required. Recent technology advances that have reduced the size and cost of "compact" cyclotrons and other high energy accelerators may facilitate increased utilization of higher energy ion irradiations in the future.

Fig. 4 provides an overview of particle energy versus penetration range for ions, electrons and neutrons in steel. The upper energy limit is set at ~100 MeV to avoid the swift heavy ion regime (and threshold nuclear reactions such as spallation for the case of protons that may induce high radioactivity and altered defect production processes). Three spatial regimes are outlined, corresponding to nanoscale near-surface displacement cascades (relevant for direct comparison of cascade features to computer simulations such molecular dynamics, but difficult or impossible to extract property changes), micron-scale intermediate ranges accessible with MeV ion irradiations (neutron-relevant microstructures for self-ions, good linkage to computational simulations, and possibility for limited nanoscale property testing) and millimeter-scale accessible with low-mass multi-MeV charged particle irradiations

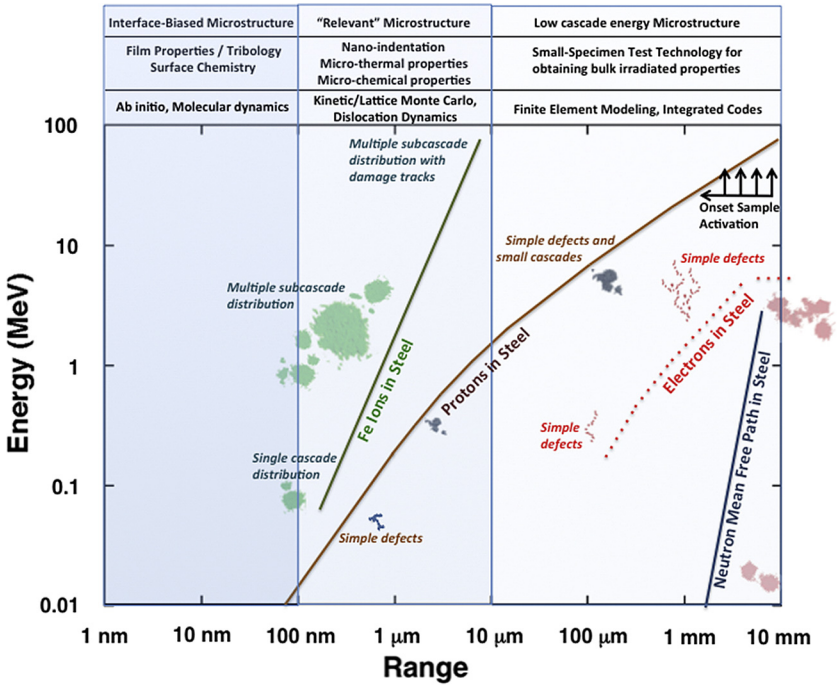

Fig. 4. Overview of particle energy vs. penetration range for ions, electrons and neutrons in steel. Considerations of neutron-relevant PKA energies, sufficient penetration depth for separation of implanted ion and near surface artifacts, capability for small-scale irradiated property measurements, and avoidance of the swift heavy ion regime highlight the potential benefits of ~10–50 MeV ion irradiations.

Please cite this article as: S.J. Zinkle, L.L. Snead, Opportunities and limitations for ion beams in radiation effects studies: Bridging critical gaps between charged particle and neut..., Scripta Materialia (2016), http://dx.doi.org/10.1016/j.scriptamat.2017.06.041

(low PKA energy cascades for light ions, but potential for obtaining bulk property changes). Electron irradiations with energies ~1–10 MeV are useful for some fundamental radiation effects studies [2,119], and they offer an additional potential advantage of providing bulk irradiated materials properties data such as tensile strength and uniform elongation since the range of electrons in steel at these energies is ~1 mm. However, due to their low mass, electrons can only transfer ~50–300 eV to the host atoms during collisions and therefore cannot simulate the energetic displacement cascades that are typical for in-core nuclear reactor applications.

Energetic self-ion irradiations offer several advantages for fundamental studies of radiation effects in materials, including the possibility to examine the microstructures of energetic displacement cascades and quantitatively compare the observations with predictions from multiscale computer simulations at similar length scales. As previously discussed, the somewhat broad distribution in cascade energies for intermediate and high-energy Fe ions as compared to that of neutrons is of potential concern, but the ability to quantitatively examine the detailed cascade structure is important for eventually settling whether or not this effect is of practical importance. A larger question regarding intermediate mass ions is the benefit of moving from intermediate to high energy. As illustrated in Fig. 4, while increasing the self-ion energy from 2 – 5 MeV to 10–50 MeV will provide a much larger intermediate-depth irradiated region (with roughly neutron-relevant PKA aspects) for microstructural characterization without near-surface or implanted ion artifacts, mechanical and physical property testing will continue to be limited to the micron-scale. Alternatively, by decreasing the mass of the ion while increasing ion energy a complementary regime can be accessed whereby lower-energy displacement cascade microstructures and extended irradiated ranges (~10 μm–1 mm) more appropriate for acquiring material engineering properties can be achieved. A disadvantage of lower mass ions is that they produce fewer displacements per ion, so the beam current must be greatly increased in order to achieve high doses in a reasonable time period (creating problematic heat removal and temperature control issues). The bounding example shown in Fig. 4 is that of protons in steel where current state of the art small specimen test technologies could be utilized to provide engineering-relevant tensile and fracture properties on through-thickness irradiated samples up to moderate doses.

5. Summary and conclusions

Ion irradiations offer indispensible scientific value for understanding specific aspects of the typically very complex radiation effects phenomena in materials. Indeed, in many aspects ion beams are better suited for these fundamental scientific studies than neutron irradiations due to generally superior experimental control and accessibility during irradiation as well as the ability to individually vary key experimental parameters such as ion energy, flux and ion species in order to systematically explore single-effects parameters such as PKA spectrum, dose rate and temperature. Ion beams generally offer advantages for in-situ irradiation microstructural and chemical studies compared to neutron irradiations.

However, in general it is not possible for accelerated damage rate ion beam experiments to simultaneously achieve all aspects of the microstructure associated with lower dose rate neutron irradiation conditions, due to the wider range of PKA spectra (in particular more pronounced probability of low energy collisions), higher ionization per dpa, dose rate effects, and near-surface and injected ion phenomena present for typical ion irradiation conditions. The higher proportion of low energy PKA events for ion irradiations increases the primary defect production efficiency whereas the increased ionization (in nonmetals) and/or subthreshold collisions may enhance point defect recombination; this can lead to either an increase or decrease in defect accumulation compared to neutron irradiation depending on detailed experimental conditions. Similarly, the effects of dose rate on microstructural evolution are predicted to be different for the various microstructural components, so that a single "temperature shift" cannot be generally applied to compensate for dose rate effects. Because of these differences in radiation phenomena, "emulation" or "simulation" of neutron irradiation conditions is generally only possible to be achieved over a limited range of ion beam conditions. The most important current roles for ion beam studies are to provide experimental validation for models, improve our understanding of fundamental radiation effects phenomena, and evaluate the general radiation tolerance of candidate engineering materials over a wide range of relevant environmental conditions.

Many studies have used ion beams of insufficient energy to explore certain radiation effects phenomena such as high dose void swelling behavior, and consequently the reported data are of questionable quantitative value without additional analysis. Near-surface defect free zones and possible peak swelling or enhanced vacancy loop formation regions immediately adjacent to the denuded zones are generally observed in all irradiated materials. The width of this near-surface zone increases with increasing temperature and decreasing damage rate ($\Delta x_v \sim (D_v/P)^{1/4}$ for recombination-dominant irradiation conditions that are frequently valid for void swelling conditions), and can approach widths ~1 μm at high temperatures. The subsurface regions near the peak displacement damage region should be avoided due to potential artifacts associated with the injected ions that produce an imbalance in the interstitial vs. vacancy supersaturation concentration. For elevated temperature and/or high dose irradiations it is particularly important to consider diffusional broadening of the as-implanted ion concentration; under some common irradiation conditions, this can lead to a doubling or larger spread of the as-implanted ion distribution.

Based on considerations of potential artifacts associated with near-surface regions and injected ion regions, along with avoidance of ion track damage phenomena that emerge at high electronic stopping powers associated with energetic heavy ions (swift heavy ion regime), particularly desirable ion irradiation conditions occur at ~10–50 MeV ion energies for medium mass self-ions and light ions.

Acknowledgement

This work was supported by the Office of Fusion Energy Sciences, U.S. Department of Energy (Grant No. DE-SC0006661 for SJZ).

References

[1] R.S. Nelson, D.J. Mazey, J.A. Hudson, J. Nucl. Mater. 37 (1970) 1–12.
[2] D.I.R. Norris, J. Nucl. Mater. 40 (1971) 66–76.
[3] J.O. Stiegler (Ed.), Proc. Workshop on Correlation of Neutron and Charged Particle Damage, CONF-760673, TN: Oak Ridge National Laboratory, Oak Ridge 1976, pp. 1–376.
[4] G.S. Was, Fundamentals of Radiation Materials Science, Springer, New York, 2007.
[5] G.S. Was, J. Mater. Res. 30 (2015) 1158–1182.
[6] E. Wakai, K. Kikuchi, S. Yamamoto, T. Aruga, M. Ando, H. Tanigawa, T. Taguchi, T. Sawai, K. Oka, S. Ohnuki, J. Nucl. Mater. 318 (2003) 267–273.
[7] M. Nastasi, J.W. Mayer, Y.Q. Wang, Ion Beam Analysis: Fundamentals and Applications, CRC Press, 2014.
[8] M.L. Taheri, E.A. Stach, I. Arslan, P.A. Crozier, B.C. Kabius, T. LaGrange, A.M. Minor, S. Takeda, M. Tanase, J.B. Wagner, R. Sharma, Ultramicroscopy 170 (2016) 86–95.
[9] K. Mo, D. Yun, Y.B. Miao, X. Liu, M. Pellin, J. Almer, J.S. Park, J.F. Stubbins, S.F. Zhu, A.M. Yacout, Materials 9 (2016) 15 11 pp.
[10] J.A. Hinks, Nucl. Instrum. Meth. B 267 (2009) 3652–3662.
[11] M. Kiritani, T. Yoshiie, S. Kojima, Y. Satoh, Radiat. Eff. Defects Solids 113 (1990) 75–96.
[12] S. Ishino, J. Nucl. Mater. 251 (1997) 225–236.
[13] J. Marian, B.D. Wirth, A. Caro, B. Sadigh, G.R. Odette, J.M. Perlado, T. Diaz de la Rubia, Phys. Rev. B 65 (2002) (144102 pp).
[14] K. Arakawa, M. Hatanaka, H. Mori, K. Ono, J. Nucl. Mater. 329-333 (2004) 1194–1198.
[15] E. Dechaumphai, J.L. Barton, J.R. Tesmer, J. Moon, Y.Q. Wang, G.R. Tynan, R.P. Doerner, R.K. Chen, J. Nucl. Mater. 455 (2014) 56–60.
[16] J. Pakarinen, M. Khafizov, L.F. He, C. Wetteland, J. Gan, A.T. Nelson, D.H. Hurley, A. El-Azab, T.R. Allen, J. Nucl. Mater. 454 (2014) 283–289.
[17] R. Cheaito, C.S. Gorham, A. Misra, K. Hattar, P.E. Hopkins, J. Mater. Res. 30 (2015) 1403–1412.
[18] F. Hofmann, D.R. Mason, J.K. Eliason, A.A. Maznev, K.A. Nelson, S.L. Dudarev, Sci Rep 5 (2015) 16042 7 pp.

Please cite this article as: S.J. Zinkle, L.L. Snead, Opportunities and limitations for ion beams in radiation effects studies: Bridging critical gaps between charged particle and neut..., Scripta Materialia (2016), http://dx.doi.org/10.1016/j.scriptamat.2017.06.041

[19] W.C. Oliver, G.M. Pharr, MRS Bull. 35 (2010) 897–907.
[20] P. Hosemann, C. Shin, D. Kiener, J. Mater. Res. 30 (2015) 1231–1245.
[21] R.S. Averback, J. Nucl. Mater. 216 (1994) 49–62.
[22] R.E. Stoller, in: R.J.M. Konings (Ed.), Comprehensive Nuclear Materials, Vol. 1, Elsevier, Amsterdam 2012, pp. 293–332.
[23] S.J. Zinkle, J. Nucl. Mater. 219 (1995) 113–127.
[24] R. Devanathan, K.E. Sickafus, W.J. Weber, M. Nastasi, J. Nucl. Mater. 253 (1998) 113–119.
[25] K. Yasuda, C. Kinoshita, R. Morisaki, H. Abe, Philos. Mag. A 78 (1998) 583–598.
[26] S.J. Zinkle, Radiat. Eff. Defects Solids 148 (1999) 447–477.
[27] Y. Zhang, R. Sachan, O.H. Pakarinen, M.F. Chisholm, P. Liu, H. Xue, W.J. Weber, Nat. Commun. 6 (2015) 8049.
[28] A. Tenenbaum, N.V. Doan, Philos. Mag. 35 (1977) 379–403.
[29] Y. Satoh, T. Sohtome, H. Abe, Y. Matsukawa, S. Kano, Philos. Mag. 97 (2017) 638–656.
[30] E. Getto, Z. Jiao, A.M. Monterrosa, K. Sun, G.S. Was, J. Nucl. Mater. 465 (2015) 116–126.
[31] J.G. Gigax, E. Aydogan, T. Chen, D. Chen, L. Shao, Y. Wu, W.Y. Lo, Y. Yang, F.A. Garner, J. Nucl. Mater. 465 (2015) 343–348.
[32] E.H. Lee, N.H. Packan, L.K. Mansur, J. Nucl. Mater. 117 (1983) 123–133.
[33] E.P. Simonen, N.M. Ghoniem, N.H. Packan, J. Nucl. Mater. 122 (1984) 391–401.
[34] H. Trinkaus, H. Ullmaier, J. Nucl. Mater. 307-311 (2002) 1705–1709.
[35] N.H. Packan, K. Farrell, J.O. Stiegler, J. Nucl. Mater. 78 (1978) 143–155.
[36] L.K. Mansur, J. Nucl. Mater. 216 (1994) 97–123.
[37] R.M. Mayer, J. Nucl. Mater. 95 (1980) 100–107.
[38] G.S. Was, Z. Jiao, E. Getto, K. Sun, A.M. Monterrosa, S.A. Maloy, O. Anderoglu, B.H. Sencer, M. Hackett, Scr. Mater. 88 (2014) 33–36.
[39] J.L. Seran, J.M. Dupouy, in: H.R. Brager, J.S. Perrin (Eds.), 11th Int. Symp. on Effects of Radiation on Materials, ASTM STP 782, American Society for Testing and Materials, Philadelphia 1982, pp. 5–16.
[40] T. Okita, T. Sato, N. Sekimura, F.A. Garner, L.R. Greenwood, J. Nucl. Mater. 307 (2002) Pii s0022-3115(02)01202-3 322-326.
[41] F.A. Garner, in: R.J.M. Konings (Ed.), Comprehensive Nuclear Materials, Vol. 4, Elsevier, Amsterdam 2012, pp. 33–95.
[42] T. Okita, T. Sato, N. Sekimura, T. Iwai, F.A. Garner, J. Nucl. Mater. 367 (2007) 930–934.
[43] J.G. Gigax, T. Chen, H. Kim, J. Wang, L.M. Price, E. Aydogan, S.A. Maloy, D.K. Schreiber, M.B. Toloczko, F.A. Garner, L. Shao, J. Nucl. Mater. 482 (2016) 257–265.
[44] B. Vigeholm, M.J. Makin, Physica Stat. Sol. 12 (1965) 877–890.
[45] M.J. Makin, Philos. Mag. 20 (1969) 1133–1146.
[46] S.J. Zinkle, in: R.E. Stoller, A.S. Kumar, D.S. Gelles (Eds.), 15th Int. Symp. on Effects of Radiation on Materials, ASTM STP 1125, American Society for Testing and Materials, Philadelphia 1992, pp. 749–763.
[47] K. Farrell, J.T. Houston, J. Nucl. Mater. 35 (1970) 352–355.
[48] J.B. Whitley, G.L. Kulcinski, P. Wilkes, H.V. Smith Jr., J. Nucl. Mater. 79 (1979) 159–169.
[49] E. Getto, K. Sun, A.M. Monterrosa, Z. Jiao, M.J. Hackett, G.S. Was, J. Nucl. Mater. 480 (2016) 159–176.
[50] N.Q. Lam, S.J. Rothman, R. Sizmann, Radiat. Eff. 23 (1974) 53–59.
[51] Y.V. Konobeev, A.V. Subbotin, V.N. Bykov, V.I. Tscherbak, Phys. Status Solidi A 29 (1975) K121–K124.
[52] J.A. Hudson, D.J. Mazey, R.S. Nelson, J. Nucl. Mater. 41 (1971) 241-.
[53] K. Farrell, J.T. Houston, A. Wolfenden, R.T. King, A. Jostons, in: J.W. Corbett, L.C. Ianniello (Eds.), Radiation-Induced Voids in Metals, National Technical Information Service, Springfield, VA 1972, pp. 376–385.
[54] W.G. Johnston, J.H. Rosolowski, A.M. Turkalo, T. Lauritzen, J. Nucl. Mater. 62 (1976) 167–180.
[55] B.N. Singh, A. Horsewell, J. Nucl. Mater. 212-215 (1994) 410–415.
[56] S.J. Zinkle, B.N. Singh, J. Nucl. Mater. 283-287 (2000) 306–312.
[57] H. Trinkaus, B.N. Singh, M. Victoria, J. Nucl. Mater. 233 (1996) 1089–1095.
[58] H. Trinkaus, H.L. Heinisch, A.V. Barashev, S.I. Golubov, B.N. Singh, Phys. Rev. B 66 (2002) (060105 pp).
[59] A. Barbu, C.S. Becquart, J.L. Bocquet, J.D. Torre, C. Domain, Philos. Mag. 85 (2005) 541–547.
[60] M.P. Short, D.R. Gaston, M. Jin, L. Shao, F.A. Garner, J. Nucl. Mater. 471 (2016) 200–207.
[61] S.L. Dudarev, A.A. Semenov, C.H. Woo, Phys. Rev. B 67 (2003) (094103 pp).
[62] M.J. Aliaga, R. Schaublin, J.F. Loffler, M.J. Caturla, Acta Mater. 101 (2015) 22–30.
[63] S.J. Zinkle, Nucl. Instrum. Meth. B 91 (1994) 234–246.
[64] S.J. Zinkle, L.L. Snead, Nucl. Instrum. Meth. B 116 (1996) 92–101.
[65] S.J. Zinkle, L.L. Snead, W.S. Eatherly, J.W. Jones, D.K. Hensley, in: S.J. Zinkle, G.E. Lucas, R.C. Ewing, J.S. Williams (Eds.), Microstructural Processes During Irradiation, Vol. 540, Materials Research Society, Warrendale, PA 1999, pp. 305–310.
[66] C.J. McHargue, G.C. Farlow, C.W. White, J.M. Williams, B.R. Appleton, H. Naramoto, Mater. Sci. Eng. 69 (1985) 123–127.
[67] L.M. Wang, R.A. Dodd, G.L. Kulcinski, Ultramicroscopy 29 (1989) 284–290.
[68] O. Tissot, C. Pareige, E. Meslin, B. Decamps, J. Henry, Mater. Res. Lett. 5 (2017) 117–123.
[69] J.B. Whitley, G.L. Kulcinski, H.V. Smith Jr., P. Wilkes, in: J.A. Sprague, D. Kramer (Eds.), Effects of Radiation on Structural Materials, American Society for Testing and Materials, Philadelphia 1979, pp. 125–142.
[70] F.A. Garner, J. Nucl. Mater. 117 (1983) 177–197.
[71] B. Badger Jr., D.L. Plumton, S.J. Zinkle, R.L. Sindelar, G.L. Kulcinski, R.A. Dodd, W.G. Wolfer, in: F.A. Garner, J.S. Perrin (Eds.), 12th Int. Symp. on Effects of Radiation on Materials, Vol. I, ASTM STP 870, Vol. I, American Society for Testing and Materials, Philadelphia 1985, pp. 297–316.
[72] E. Getto, Z. Jiao, A.M. Monterrosa, K. Sun, G.S. Was, J. Nucl. Mater. 462 (2015) 458–469.
[73] E.H. Lee, L.K. Mansur, M.H. Yoo, J. Nucl. Mater. 85&86 (1979) 577–581.
[74] L.K. Mansur, Nucl. Technol. 40 (1978) 5–34.
[75] D.L. Plumton, W.G. Wolfer, J. Nucl. Mater. 120 (1984) 245–253.
[76] D.L. Plumton, G.L. Kulcinski, J. Nucl. Mater. 133 (1985) 444–447.
[77] J.F. Ziegler, J.P. Biersak, U. Littmark, The Stopping and Range of Ions in Solids, Pergamon Press, New York, 1985.
[78] R. Sizmann, J. Nucl. Mater. 69&70 (1978) 386–412.
[79] A. Müller, V. Naundorf, M.P. Macht, J. Appl. Phys. 64 (1988) 3445–3455.
[80] A.I. Van Sambeek, R.S. Averback, C.P. Flynn, M.H. Yang, in: I.M. Robertson, L.E. Rehn, S.J. Zinkle, W.J. Phythian (Eds.), Microstructure of Irradiated Materials, Vol. 373, Materials Research Society, Pittsburgh 1995, pp. 293–298.
[81] N.D. Evans, S.J. Zinkle, J. Bentley, in: I.M. Robertson, L.E. Rehn, S.J. Zinkle, W.J. Phythian (Eds.), Microstructure of Irradiated Materials, Vol. 373, Materials Research Society, Pittsburgh 1995, pp. 419–424.
[82] F.A. Smidt Jr., P.R. Malmberg, J.A. Sprague, J.E. Westmoreland, in: F.R. Schober, J.A. Sprague (Eds.), Irradiation Effects on the Microstructure and Properties of Metals, ASTM STP 611, American Society for Testing and Materials, Philadelphia 1976, pp. 227–241.
[83] M.B. Toloczko, F.A. Garner, V.N. Voyevodin, V.V. Bryk, O.V. Borodin, V.V. Mel'nychenko, A.S. Kalchenko, J. Nucl. Mater. 453 (2014) 323–333.
[84] E. Aydogan, T. Chen, J.G. Gigax, D. Chen, X. Wang, P.S. Dzhumaev, O.V. Emelyanova, M.G. Ganchenkova, B.A. Kalin, M. Leontiva-Smirnova, R.Z. Valiev, N.A. Enikeev, M.M. Abramova, Y. Wu, W.Y. Lo, M. Yang, M.P. Short, S.A. Maloy, F.A. Garner, L. Shao, J. Nucl. Mater. 482 (2017) 96–104.
[85] X. Wang, A.M. Monterrosa, F.F. Zhang, H. Huang, Q.Z. Yan, Z.J. Jiao, G.S. Was, L.M. Wang, J. Nucl. Mater. 462 (2015) 119–125.
[86] D.I.R. Norris, Radiat. Eff. 15 (1972) 1–22.
[87] F.A. Garner, L.E. Thomas, in: J. Moteff (Ed.), Effects of Radiation on Substructure and Mechanical Properties of Metals and Alloys, American Society for Testing and Materials, Philadelphia 1973, pp. 303–323.
[88] J. Wang, M.B. Toloczko, N. Bailey, F.A. Garner, J. Gigax, L. Shao, Nucl. Instrum. Meth. B 387 (2016) 20–28.
[89] M.L. Lescoat, J. Ribis, Y. Chen, E.A. Marquis, E. Bordas, P. Trocellier, Y. Serruys, A. Gentils, O. Kaitasov, Y. de Carlan, A. Legris, Acta Mater. 78 (2014) 328–340.
[90] H.S. Carslaw, J.C. Jaeger, Conduction of Heat in Solids, Oxford University Press, 1959.
[91] F.A. Garner, M.B. Toloczko, B.H. Sencer, J. Nucl. Mater. 276 (2000) 123–142.
[92] T. Iwata, A. Iwase, Nucl. Instrum. Meth. B 61 (1991) 436–440.
[93] A. Dunlop, D. Lesueur, Mater. Sci. Forum 97-99 (1992) 553–576.
[94] H. Dammak, A. Barbu, A. Dunlop, D. Lesueur, N. Lorenzelli, Philos. Mag. Lett. 67 (1993) 253–259.
[95] A. Dunlop, D. Lesueur, P. Legrand, H. Dammak, Nucl. Instrum. Meth. Phys. Res. B 90 (1994) 330–338.
[96] Z.G. Wang, C. Dufour, E. Paumier, M. Toulemonde, J. Phys. Condens. Matter 6 (1994) 6733–6750.
[97] H. Dammak, A. Dunlop, D. Lesueur, Nucl. Instrum. Meth. Phys. Res. B 107 (1996) 204–211.
[98] A. Iwase, S. Ishino, J. Nucl. Mater. 276 (2000) 178–185.
[99] G. Szenes, Z.E. Horvath, B. Pecz, F. Paszti, L. Toth, Phys. Rev. B 65 (2002) (045206 pp).
[100] W. Wesch, A. Kamarou, E. Wendler, Nucl. Instrum. Meth. B 225 (2004) 111–128.
[101] A. Benyagoub, A. Audren, L. Thome, F. Garrido, Appl. Phys. Lett. 89 (2006) 241914 3 pp.
[102] M. Toulemonde, S. Bouffard, F. Studer, Nucl. Instrum. Meth. B 91 (1994) 108–123.
[103] G. Szenes, Phys. Rev. B 60 (1999) 3140–3147.
[104] M. Toulemonde, C. Dufour, A. Meftah, E. Paumier, Nucl. Instrum. Meth. B 166-167 (2000) 903–912.
[105] S.J. Zinkle, V.A. Skuratov, D.T. Hoelzer, Nucl. Instrum. Meth. B 191 (2002) 758–766.
[106] M. Toulemonde, W. Assmann, C. Dufour, A. Meftah, F. Studer, C. Trautmann, in: P. Sigmund (Ed.), Ion Beam Science: Solved and Unsolved Problems, Pts 1 and 2, Vol. 52, Royal Danish Academy Sciences & Letters, Copenhagen V 2006, pp. 263–292.
[107] M. Lang, R. Devanathan, M. Toulemonde, C. Trautmann, Curr. Opin. Solid State Mater. Sci. 19 (2015) 39–48.
[108] H. Schroeder, H. Ullmaier, J. Nucl. Mater. 179-181 (1991) 118–124.
[109] Z. Zhu, P. Jung, J. Nucl. Mater. 212-215 (1994) 1081–1086.
[110] A. Hasegawa, M. Ejiri, S. Nogami, M. Ishiga, R. Kasada, A. Kimura, K. Abe, S. Jitsukawa, J. Nucl. Mater. 386-388 (2009) 241–244.
[111] H. Ullmaier, F. Carsughi, Nucl. Instrum. Meth. B 101 (1995) 406–421.
[112] J. Chen, H. Ullmaier, T. Flossdorf, W. Kühnlein, R. Duwe, F. Carsughi, T. Broome, J. Nucl. Mater. 298 (2001) 248–254.
[113] M. Victoria, N. Baluc, C. Bailat, Y. Dai, M.I. Luppo, R. Schäublin, B.N. Singh, J. Nucl. Mater. 276 (2000) 114–122.
[114] T. Wiss, H. Matzke, C. Trautmann, M. Toulemonde, S. Klaumünzer, Nucl. Instrum. Meth. B 122 (1997) 583–588.
[115] H. Matzke, P.G. Lucuta, T. Wiss, Nucl. Instrum. Meth. B 166-167 (2000) 920–926.
[116] T. Wiss, H. Matzke, Radiat. Meas. 31 (1999) 507–514.
[117] S.J. Zinkle, H. Matzke, V.A. Skuratov, in: S.J. Zinkle, G.E. Lucas, R.C. Ewing, J.S. Williams (Eds.), Microstructural Processes During Irradiation, Vol. 540, Materials Research Society, Warrendale, PA 1999, pp. 299–304.
[118] M. Lang, J. Lian, F.X. Zhang, B.W.H. Hendriks, C. Trautmann, R. Neumann, R.C. Ewing, Earth Planet. Sci. Lett. 274 (2008) 355–358.
[119] M. Kiritani, Ultramicroscopy 39 (1991) 180–186.

Please cite this article as: S.J. Zinkle, L.L. Snead, Opportunities and limitations for ion beams in radiation effects studies: Bridging critical gaps between charged particle and neut..., Scripta Materialia (2016), http://dx.doi.org/10.1016/j.scriptamat.2017.06.041